Title
Ab initio study of low energy electron collisions with ethylene

Journal
Physical Review A, 68(62707)

Authors
Trevisan, C.S.
Orel, A.E.
Rescigno, T.N.

Publication Date
2003-10-06

AB INITIO STUDY OF LOW-ENERGY ELECTRON COLLISIONS WITH ETHYLENE

C. S. Trevisan,[1] A. E. Orel,[1] and T. N. Rescigno[2]

[1]*Department of Applied Science, University of California, Davis, CA 95616*
[2]*Lawrence Berkeley National Laboratory, Computing Sciences, Berkeley, California 94720*

We present the results of an investigation of elastic electron scattering by ethylene, C_2H_4, with incident electron energies ranging from 0.5 to 20 eV, using the complex Kohn variational method. These are the first fully *ab initio* calculations to accurately reproduce experimental angular differential cross sections at energies below 3 eV. Low-energy electron scattering by ethylene is sensitive to the inclusion of electronic correlation and target-distortion effects. We therefore report results that describe the dynamic polarization of the target by the incident electron and involve calculations over a range of different geometries, including the effects of nuclear motion in the resonant $^2B_{2g}$ symmetry with an adiabatic nuclei treatment of the C-C stretch mode. The inclusion of dynamic polarization and the effect of nuclear motion are equally critical in obtaining accurate results. The calculated cross sections are compared with recent experimental measurements.

PACS numbers: 34.80.Gs

I. INTRODUCTION

Collisions of electrons with small polyatomic molecules are important in many areas of physics. They are of interest in determining the energy balance and transport properties of electrons in low-temperature gases and plasmas under a wide variety of conditions. Electron-molecule collision data is critically important for numerical modeling studies [1] in wide-ranging areas such as plasma deposition and etching of semiconductors, gaseous high voltage switches and environmental remediation plasmas.

Electron scattering by hydrocarbons is particularly relevant to cold plasma technology. Although ethylene, C_2H_4, is one of the simpler hydrocarbon molecules, there have been only very limited studies of its interaction with low-energy electrons.

Low-energy electron scattering by atoms and molecules can be dominated by electrostatic interaction effects, electron exchange, and electron correlation. The proper balance of these effects is needed to theoretically describe effects such as the Ramsauer-Townsend (RT) effect. Shape resonances are also sensitive to the effects of electron correlation and, in addition, are sensitive to changes in target nuclear geometry. The proper inclusion of all these factors is crucial for an adequate description of resonance parameters and vibrational excitation cross sections.

We present the results of an investigation of the collision of low-energy electrons with ethylene using the complex Kohn variational method. Ethylene is a closed-shell molecule which possesses a permanent quadrupole moment. Early *ab initio* calculations by Schneider *et al.* [2] were the first to confirm the existence of the Ramsauer-Townsend effect in such a molecule. Ethylene also has a low-lying shape resonance whose position and width are strongly influenced by target-distortion effects. The resonance is of $^2B_{2g}$ symmetry and corresponds to the temporary capture of the incident electron into an empty, antibonding, valence orbital. The investigations of Schneider *et al.* , which were carried out only at the equilibrium geometry and included only two scattering symmetries, produced a resonance at 1.83 eV, in excellent agreement with experiment. Several other theoretical studies on low-energy electron scattering from ethylene have been performed in the fixed-nuclei approximation at equilibrium geometry[3–5]. None of the previous calculations, however, have been particularly successful in describing experimental angular differential cross sections at electron impact energies below 3 eV, as evidenced by the recent experimental measurements of Panajotovic *et al.* [6].

The present calculations extend the work of Schneider *et al.* [2] by including all relevant symmetries and important dynamical correlation effects. In addition, the calculations include the effects of nuclear motion for the critically important resonant symmetry. It will be shown below that all these factors are essential in obtaining accurate total, momentum transfer, and elastic differential cross sections.

II. THEORETICAL FORMULATION

The complex Kohn method is a variational technique which uses a trial wave function that is expanded in terms of square-integrable (Cartesian Gaussian) and continuum basis functions that incorporate the correct asymptotic boundary conditions. Detailed descriptions of the method have been given in previous publications (see, for instance, refs. [7, 8]), so only a brief summary of the aspects that concern this study will be given below.

In the case of electronically elastic scattering, the trial wave function to be used is of the form:

$$\Psi = \mathcal{A}[\Phi_o(\vec{r}_1..\vec{r}_N)F(\vec{r}_{N+1})] + \sum_\mu d_\mu \Theta_\mu(\vec{r}_1..\vec{r}_{N+1}) \quad (1)$$

where Φ_o is the (Hartree-Fock) ground-state of C_2H_4, $\mathcal{A}$ antisymmetrizes the coordinates of the incident electron ($\vec{r}_{N+1}$) with those of the target electrons ($\vec{r}_1..\vec{r}_N$) and the sum contains square-integrable, $(N+1)$ - electron terms that describe polarization and/or correlation effects due to electronically closed channels. In the present study, these configuration-state functions (CSFs), Θ_μ, were constructed as products of bound molecular orbitals and terms obtained by singly exciting the target Hartree-Fock wave function. Thus the configurations in Eq. (1) have the form

$$\Theta_\mu = \mathcal{A}(\Phi_o[\phi_o \rightarrow \phi_\alpha]\phi_i) \quad (2)$$

where $\phi_o \rightarrow \phi_\alpha$ denotes the replacement of occupied orbital ϕ_o by orbital ϕ_α, and ϕ_i is another virtual orbital.

The proper construction of the correlation component of the trial wave function is critical in determining the low-energy behavior of the elastic cross sections and the position and width of shape resonances. Moreover, there are different ways in which this correlation portion of the trial wave function should be built, depending on the symmetry under consideration. These different approaches will be described throughout the sections that follow.

The scattering function, $F(\vec{r}_{N+1})$, is further expanded in the Kohn method in a combined basis of Gaussian (ϕ_i) and continuum (Ricatti-Bessel, j_l,and Hankel, h_l^+) basis functions

$$F(\vec{r}) = \sum_i c_i\phi_i(\vec{r}) + \sum_{lm}[j_l(kr)\delta_{ll_o}\delta_{mm_o} + T_{ll_omm_o}h_l^+(kr)]Y_{lm}(\hat{r})/r. \quad (3)$$

where $Y_{lm}(\hat{r})$ are spherical harmonics. Applying the stationary principle for the T-matrix,

$$T_{stat} = T_{trial} - 2\int \Psi(H-E)\Psi \quad (4)$$

results in a set of linear equations for the coefficients c_i, d_μ and $T_{ll_omm_o}$. The T-matrix elements, $T_{ll_omm_o}$, are the fundamental dynamical quantities from which all fixed-nuclei cross sections are derived.

III. THEORETICAL MODELS FOR ELECTRON-MOLECULE COLLISIONS AND CALCULATIONS

In an approach similar to that employed by Rescigno *et al.* [9] in a study of CO_2, we found that the best description of the low-energy scattering by C_2H_4 is attained when analyzing the prevailing physical processes related to each symmetry. The following subsections will briefly describe the different approximations that were considered and how they were introduced into our calculations.

Table I lists the Gaussian basis sets employed in all our scattering calculations. In every case, a self-consistent field (SCF), Hartree-Fock target wave function for the ground state of C_2H_4 was used. The target basis was augmented with additional diffuse Gaussian functions, also in Table I, for the construction of the Kohn trial wave function. The expansion of the trial scattering function was completed by including numerically generated continuum basis functions, retaining terms with angular momentum quantum numbers l and $|m|$ less than or equal to 6.

A. Static-exchange

The simplest approximation to describe an electron-molecule collision, consistent with the Pauli principle, would be to express the scattering wave function as an antisymmetrized product of the target wave function and a scattered electron function, i.e., as the first term of Eq. (1). This so-called static-exchange (SE) approximation cannot be expected to yield accurate results at collision energies (generally less than 5 eV) where target polarization is important, at least for total symmetries in which the incident electron significantly penetrates the target. The SE approximation makes no allowance for the target to relax to the presence of the scattering electron. This model can describe shape resonances, although SE results generally place their position too high and their width too broad in energy.

All symmetries in our calculations were treated beyond the SE approximation [10]. Although this level of approximation generally displays the basic features of the scattering process at higher energies, it is known to be quantitatively, and often qualitatively, incorrect at scattering energies below several eV.

B. Polarized SCF

At low energies for the incident electron, it becomes necessary to describe its dynamic polarization effect on the target. Previous work on this and other closed-shell molecules has shown that including a set of specific configurations in Eq. (1) to produce what is known as a "polarized SCF" (PSCF) trial wave function provides a good description of target polarization, with a balance of correlation effects in the N - and $(N+1)$ - electron systems [2, 9, 11–13]. In the PSCF approach [11] the CSFs, Θ_μ, are constructed from the product of bound molecular orbitals and terms obtained by singly exciting the target SCF wave function, as mentioned before. Instead of using all the unoccupied orbitals to define a space of singly excited CSFs, we choose a compact sub-

set of these virtual orbitals, the polarized virtual orbitals (ϕ_α in Eq. (2)), for singly exciting the target. These polarized orbitals are constructed following the prescription of ref. [11]. We further restricted the CSFs in the PSCF wave function by including only those single excitations that preserved the singlet spin symmetry of the ground state.

The five highest occupied orbitals were used to generate the set of polarized orbitals. The entire space of target and supplemental diffuse basis functions listed in Table I was used in the construction of the polarized orbitals. A structure calculation on the neutral target using an SCF configuration for the ground state and single excitations from these occupied orbitals into the polarized orbitals gave a polarizability (in atomic units) of 29.473 , which is 99.74% of the experimentally determined value [14]. This suggests that using an SCF description of the target is a good approximation. PSCF calculations were performed for all total symmetries with the exception of $^2B_{2g}$. The following subsection will describe the way this latter symmetry was tackled.

Ramsauer-Townsend minima are present in the elastic low-energy scattering cross sections of many closed-shell, non-polar targets. Our PSCF approach successfully describes the Ramsauer-Townsend minimum in the e^- - C_2H_4 elastic cross section that occurs in ^2A_g symmetry [2].

C. Relaxed-SCF

Another low-energy feature that characterizes e^- - C_2H_4 scattering is a shape resonance of $^2B_{2g}$ symmetry. In symmetries that include shape resonances, the PSCF model may lead to an unbalanced description of correlation in the temporary negative-ion state relative to the SCF target state at short range, with the result that the resonance will appear at too low an energy relative to the target ground state. Previous experience with a number of closed-shell target molecules has shown that a "relaxed-SCF" (RSCF) model provides a good description of symmetries that present shape resonances [2, 13, 15–17]. The key is to include in the trial function only those correlation terms that produce an orbital relaxation effect, similar to the type of relaxation that would be produced in performing an SCF calculation on the negative ion. The relaxed-SCF trial function only includes configurations Θ_μ built from single excitations of the occupied target orbitals into virtual orbitals of the same symmetry; no $\phi_o \rightarrow \phi_\alpha$ excitation that breaks the spatial symmetry of the ground state is included in the calculation. This type of trial function describes the essential short-range core relaxation effects that are needed to describe a shape resonance but does not include the long-range dipole-polarization effects of the PSCF model. We therefore constructed a relaxed-SCF trial wave function for the $^2B_{2g}$ symmetry, obtaining an accurate description of the well known low-energy resonance that

TABLE I: Gaussian basis sets used in e^- - C_2H_4 scattering calculations. Underlines separate contracted basis functions.

Center	Type	Exponent	Coefficient
Target basis			
Carbon	s	4232.610000	0.006228
Carbon	s	634.882000	0.047676
Carbon	s	146.097000	0.231439
Carbon	s	42.497400	0.789108
Carbon	s	14.189200	0.791751
Carbon	s	1.966600	0.321870
Carbon	s	5.147700	1.000000
Carbon	s	0.496200	1.000000
Carbon	s	0.153300	1.000000
Carbon	s	0.050000	1.000000
Carbon	p	18.155700	0.039196
Carbon	p	3.986400	0.244144
Carbon	p	1.142900	0.816775
Carbon	p	0.359400	1.000000
Carbon	p	0.114600	1.000000
Carbon	p	0.050000	1.000000
Carbon	d	0.750000	1.000000
Carbon	d	0.300000	1.000000
Hydrogen	s	74.690000	0.025374
Hydrogen	s	11.230000	0.189684
Hydrogen	s	2.546000	0.852933
Hydrogen	s	0.713000	1.000000
Hydrogen	s	0.224900	1.000000
Hydrogen	p	0.750000	1.000000
Diffuse scattering basis, A_g symmetry			
Center of mass	s	0.020000	1.000000
Center of mass	s	0.010000	1.000000
Center of mass	s	0.005000	1.000000
Center of mass	d	0.090000	1.000000
Center of mass	d	0.035000	1.000000
Center of mass	d	0.010000	1.000000
Diffuse scattering basis, B_{1g}, B_{2g} and B_{3g} symmetries			
Center of mass	d	0.160000	1.000000
Center of mass	d	0.080000	1.000000
Center of mass	d	0.040000	1.000000
Center of mass	d	0.020000	1.000000
Center of mass	d	0.010000	1.000000
Diffuse scattering basis, B_{1u}, B_{2u} and B_{3u} symmetries			
Center of mass	p	0.030000	1.000000
Center of mass	p	0.015000	1.000000
Center of mass	p	0.007500	1.000000
Center of mass	p	0.003750	1.000000
Center of mass	p	0.001000	1.000000

occurs in this symmetry.

IV. APPROXIMATE TREATMENT OF NUCLEAR MOTION

To date, theoretical treatments of e^- - C_2H_4 scattering have been restricted to fixed-nuclei calculations at the equilibrium geometry. Although this approach has produced total cross sections that qualitatively agree with experiment[2–5], significant disagreement remains for differential cross sections at energies below 3 eV.

One obvious source of error is the neglect of nuclear motion in the critically important resonant symmetry. To address this problem, we focused on the C-C stretch mode (labeled as $\nu_2^{CC}(a_g)$ by Herzberg [18]), which is most strongly coupled to the resonance. As in an earlier study of CO_2 [9], we used an adiabatic nuclei treatment [19] to compute a vibrationally averaged T-matrix in the resonant $^2B_{2g}$ symmetry. The other symmetries are far less sensitive to changes in nuclear geometry. We verified this by performing calculations in ^2A_g at several different geometries and found the fixed nuclei cross section to vary by 5 percent over the energy range $0.5< E <20$ eV. There are proportionately larger changes in the immediate vicinity of the RT minumum (0.18 eV), but the calculations we are reporting here do not probe this low-energy region. Symmetric-stretch motion does not break the symmetry of the target, thus the same symmetry designations can continue to be used.

The vibrationally averaged T-matrix, in B_{2g} symmetry, is computed as:

$$T_{ll'}^{av}(E) = \langle \chi_o | T_{ll'}^{B_{2g}}(E,R) | \chi_o \rangle, \tag{5}$$

where $\chi_o(R)$ is the symmetric stretch vibrational wave function and the average is taken over the C-C normal mode. Harmonic oscillator functions were used, with constants derived from Herzberg [18]. E and R denote the dependency on energy and on geometry, respectively. Without loss of clarity, we will drop these dependencies in some of the equations that follow to simplify notation.

In the eigenphase representation, $T_{ll'}^{B_{2g}}$ can be written as

$$T_{ll'}^{av} = \sum_{\lambda} c_l^{\lambda} c_{l'}^{\lambda} e^{i\delta_{\lambda}^{B_{2g}}} sin(\delta_{\lambda}^{B_{2g}}) \tag{6}$$

The mixing coefficients c_l^{λ} are elements of the unitary matrix of eigenchannel vectors that diagonalize the T-matrix and $\delta_{\lambda}^{B_{2g}}$ are the eigenphases. We found that, over a number of different geometries, the resonance behavior was clearly concentrated in one eigenphase, $\delta_{\lambda res}^{B_{2g}}$, while the other eigenphases were small and smoothly varying with energy and geometry. Therefore, with only one eigenphase varying significantly, we were able to separate out the resonant term from the sum in Eq. (6) and ignore the geometry dependence of the non-resonant contributions so as to average the resonant component only. The final expression for our T-matrix elements is given by:

$$T_{ll'}^{av} = \langle \chi_o | c_l^{\lambda_{res}} c_{l'}^{\lambda_{res}} e^{i\delta_{\lambda_{res}}^{B_{2g}}} sin(\delta_{\lambda_{res}}^{B_{2g}}) | \chi_o \rangle + \sum_{\lambda \neq \lambda_{res}} c_l^{\lambda} c_{l'}^{\lambda} e^{i\delta_{\lambda}^{B_{2g}}} sin(\delta_{\lambda}^{B_{2g}}) \tag{7}$$

We performed fixed-nuclei calculations at the equilibrium geometry of C_2H_4, as well as at two other (stretched and compressed) geometries. The fixed-nuclei $^2B_{2g}$ cross sections are shown in Fig. 1. The resonance is clearly very sensitive to changes in C-C bond distance, becoming narrower and lower in energy as the molecule is stretched. We fitted the resonant eigenphase to a Breit-Wigner form at each geometry,

$$\delta_{\lambda_{res}}^{B_{2g}}(R) = \arctan\left[\frac{\Gamma(R)}{2(E - E_{res}(R))}\right] - \arctan\left[\frac{\Gamma(R)}{-2E_{res}(R)}\right] + d_1(R)E + d_2(R)E^2 \tag{8}$$

where $\Gamma(R)$ represents the resonance width, $E_{res}(R)$ is the resonance energy and $d_i(R)$ are fitting coefficients. Both $\Gamma(R)$ and $E_{res}(R)$ were found to vary smoothly with R and were easily interpolated to give the resonant T-matrix elements at any value of R. This greatly facilitates the average required in Eq. (5). The resonance parameters are listed in Table II.

TABLE II: Parameters obtained by fitting the resonant eigenphase, $\delta_{\lambda_{res}}^{B_{2g}}$, to the Breit-Wigner form of Eq. (8) at different C-C internuclear separations, R(a_o).

R(a_o)	$\Gamma(eV)$	$E_{res}(eV)$	$d_1((eV)^{-1})$	$d_2((eV)^{-2})$
2.27808	-1.0374	2.6555	-0.0945	0.0092
2.53120	-0.4963	1.8517	-0.0735	0.0048
2.78432	-0.1576	1.1073	-0.0890	0.0106

The resonance parameters extracted from these scattering calculations give the resonance energy relative to the C_2H_4 ground state. The total electronic energy for the resonance is the resonance energy plus the C_2H_4 ground state energy. In Fig. 2, the resonance and neutral ground state potential energy curves are plotted as a function of the C-C bond distance.

V. RESULTS

Except for the $^2B_{2g}$ component, cross sections were calculated for all symmetries by a PSCF approach at the equilibrium geometry of the ground state (R_{CC} = 1.339 Å, R_{CH} = 1.086 Å, H-C-H = 117.6°), namely, symmetries A_g, B_{1g}, B_{3g}, B_{1u}, B_{2u} and B_{3u}. Symmetry A_u

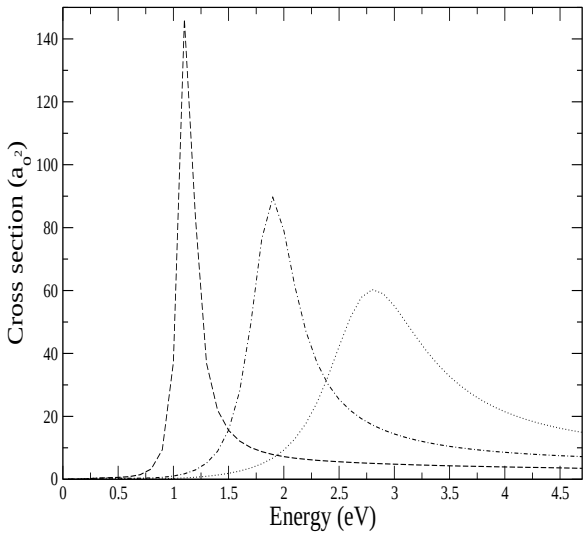

FIG. 1: Symmetric-stretch dependence of the fixed-nuclei, $^2B_{2g}$ component of the integrated cross section. The chained curve represents RSCF calculations at equilibrium geometry. The dotted curve represents a symmetric compression to a C-C bond distance of 2.27808. Dashed curve: symmetric stretch to a C-C bond distance of 2.78432. Cross sections are given in atomic units. ($1a_o^2$ = 2.8 x 10^{-17} cm^2)

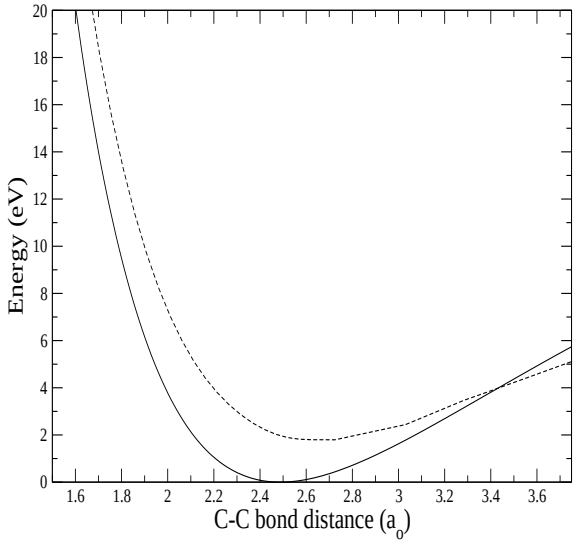

FIG. 2: Potential energy curves for $^2B_{2g}$ negative ion resonance (dashed curve) and neutral ground state (solid curve) as a function of C-C bond distance.Bond distance is plotted in atomic units ($1a_o$ = 0.529 x 10^{-8} cm)

was found to be unimportant at low energy and was left out of the calculations.

The total elastic and momentum transfer cross sections are plotted in Fig. 3 along with recent measurements and the Schwinger variational results of Brescansin *et al.* [5] which used a model polarization potential. The experimental values were obtained by Panajotovic *et al.* [6] on two different crossed-beam electron spectrometers: open circles refer to measurements at the Australian National University (ANU), while diamonds represent measurements performed at Sophia University, Japan (Sophia). It is clear that the inclusion of nuclear motion is necessary to properly describe the cross sections in the resonance region.

At energies near and below the resonance peak, the cross sections are sensitive to the effects of both geometry and dynamic correlation. This is most clearly seen in the angular differential cross sections. Fig. 4 illustrates this sensitivity at 2 eV incident electron energy, which is near the center of the resonance at equilibrium geometry. The figure includes a solid curve which represents results that incorporate an adiabatic-nuclei treatment of symmetric stretch motion and a dashed curve that describes the present results without the inclusion of nuclear motion, at equilibrium geometry. The chained curve, which corresponds to a preliminary SE treatment of all symmetries (also at equilibrium geometry) except A_g (treated by PSCF) and B_{2g} (RSCF) [10] is included to illustrate the sensitivity of differential cross sections to geometry and correlation effects. The fact that the A_g and B_{2g} symmetries are sensitive to correlation effects is not suprising, since there is a Ramsauer-Townsend minimum and a shape resonance in these symmetries, respectively. We also found that the non-resonant B_{1u}, B_{2u} and B_{3u} symmetries, which have leading p-wave behavior, significantly penetrate the target at low energies and are sensitive to dynamic correlation. In the resonance region, the cross sections are particularly sensitive to effects which can change the resonance position. To illustrate this, we performed RSCF calculations in B_{2g} symmetry in which half the correlating configurations (specifically, the singlet-triplet target excitations) were dropped, which shifts the resonance position upward by 0.5 eV. Those results are shown as the dashed curve in Fig. 4. Clearly, getting accurate differential cross sections in the resonance region requires calculations that put the resonance at the right energy.

Figures 5 and 6 show elastic angular differential cross sections at different incident energies. We plot curves that represent calculations both with and without the inclusion of nuclear motion, represented by the solid and dashed curves, respectively. We also show theoretical re-

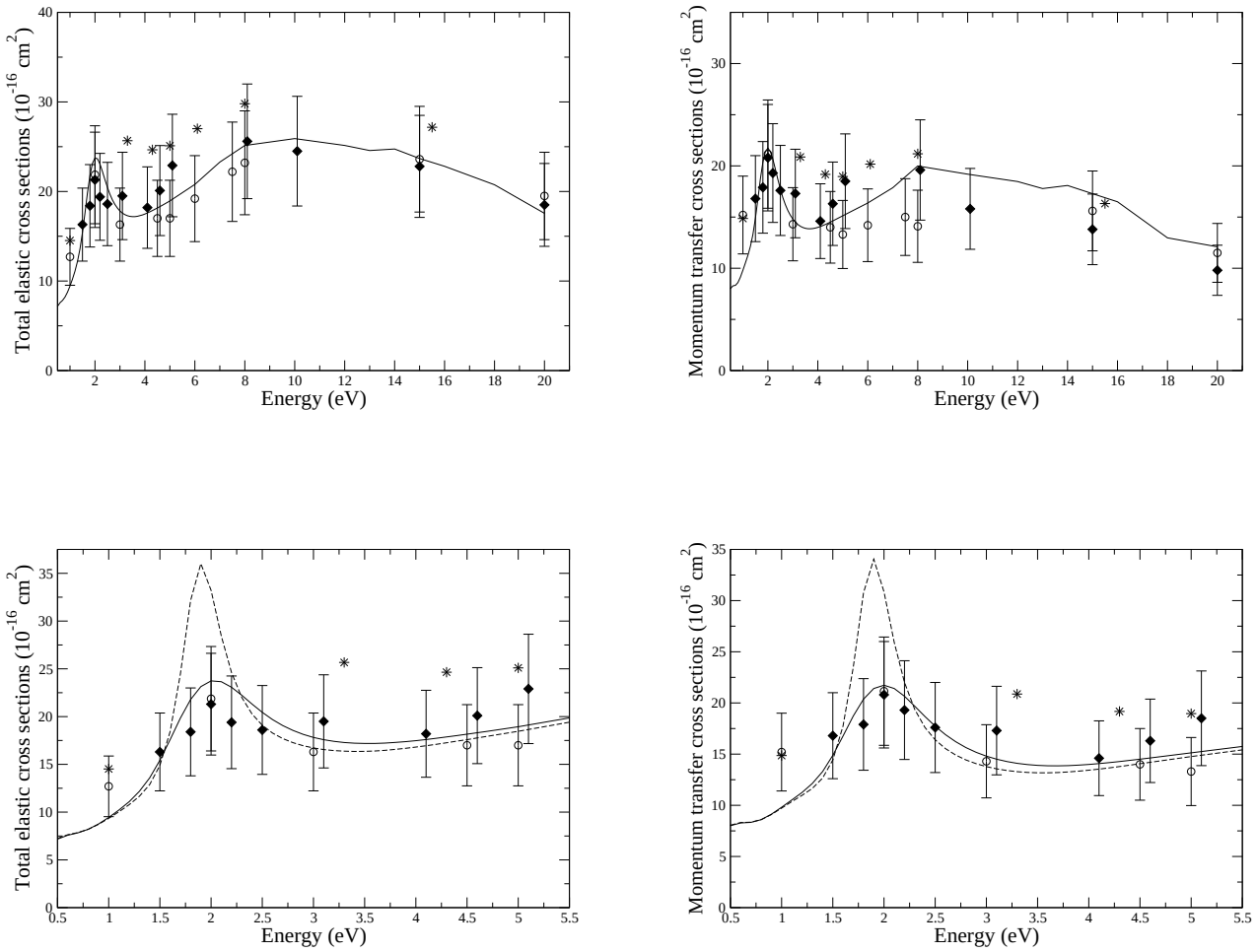

FIG. 3: Total elastic and momentum transfer cross sections for e - C_2H_4 scattering. Solid curve: present results which incorporate an adiabatic-nuclei treatment of symmetric stretch motion. Dashed curve: present results without the inclusion of nuclear motion, at equilibrium geometry. Open circles: Panajotovic *et al.* 's ANU measurements [6]. Diamonds: Panajotovic *et al.* 's Sophia measurements [6]. Stars: theoretical results of Brescansin *et al.* [5].

sults of Brescansin *et al.* [5] at available energies for comparison. Note that the calculations of Brescansin *et al.* plotted at 3.0, 4.5, 6.0 and 15.0 eV were actually performed at energies of 3.3, 4.3, 6.1 and 15.5 eV. Again, the experimental measurements are those of Panajotovic *et al.* . It is worth noting that there are differences of approximately 20 to 30% between the data obtained by these two different experimental apparatii. These differences are particularly noticeable at small scattering angles, where the cross sections appear to follow different trends. At energies below 3 eV, our calculations appear to agree better with the ANU data than with the Sophia measurements. Vibrational averaging is clearly important at 1.8 and 2.0 eV, which are close to the resonance peak, and significantly improve the comparison with experiment. The effects of nuclear motion become less important at energies outside the resonance region. The principal effect of nuclear averaging is, not surprisingly, to reduce the magnitude of the cross sections without significantly affecting their shape. At energies of 3 eV and above, our cross sections are in very good agreement with experiment. For energies below 5.0 eV, the results of Brescansin *et al.* are systematically too high at small scattering angles, while at 5.0 eV and above there is good mutual agreement. At these higher energies, the results also agree with the static-exchange results of Winstead *et al.* [4, 6] (not shown).

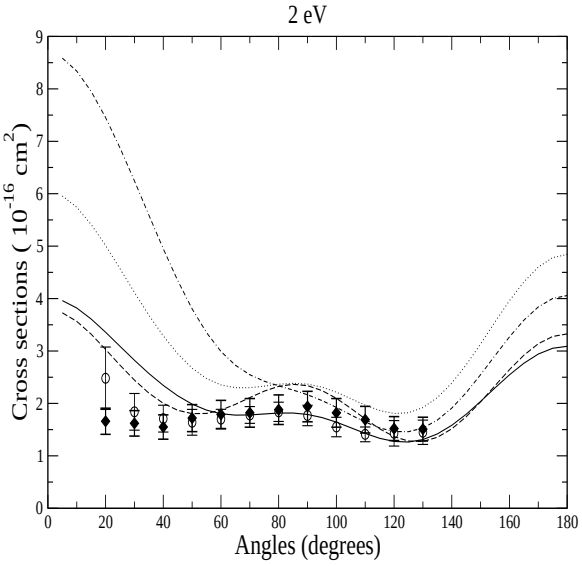

FIG. 4: Elastic differential cross sections for e - C_2H_4 scattering at incident energy of 2 eV. Solid curve: present results which incorporate an adiabatic-nuclei treatment of symmetric stretch motion. Dotted curve: present results without the inclusion of nuclear motion, at equilibrium geometry. Dashed curve: present results without the inclusion of nuclear motion, at equilibrium geometry, and a partial treatment of relaxation in B_{2g} symmetry. The chain curve represents SE calculations at equilibrium geometry for symmetries other than A_g and B_{2g}. Open circles: Panajotovic *et al.* 's ANU measurements [6]. Diamonds: Panajotovic *et al.* 's Sophia measurements [6].

VI. CONCLUSIONS

We have carried out a variational treatment of electronically elastic $e^- - C_2H_4$ scattering. At low energies, we found a strong sensitivity of the cross sections to the effects of both geometry and dynamic correlation. A polarized-SCF approach was used for all symmetries except for the resonant component $^2B_{2g}$, for which we found a relaxed-SCF method more appropriate. For the resonant symmetry, we also included an approximate treatment of nuclear motion by using a simple adiabatic treatment of the symmetric stretch (C-C) vibrational mode.

It is interesting to note that there are no oscillatory structures observed in the elastic cross sections in the vicinity of the $^2B_{2g}$ resonance, either in the Panajotovic *et al.* measurements [6] or in the high resolution experiments of Allan [20]. This might seem surprising, since such structures are well known in the case of N_2, which has a similar reduced mass and very similar resonance properties (near equilibrium geometry) [16]. The difference here is that, as seen from Fig. 2, a wavepacket originally centered on the resonance curve near the equilibrium geometry of the neutral (corresponding to a C-C distance of 2.53 a_o), would be largely confined by energy conservation to C-C distances less than 3.0 a_o. Over this range of geometries, the resonance width is substantial and the wavepacket decays too rapidly to produce the kind of "boomerang" structure observed in the case of molecular nitrogen.

Both of the main low-energy features of this electron-molecule system were successfully described by these calculations, namely, the Ramsauer-Townsend minimum in ^2A_g symmetry and the $^2B_{2g}$ shape resonance. The integrated elastic and momentum transfer cross sections we obtained are in excellent agreement with recent experiments. We have also found that the effects included in this treatment significantly improve the agreement with measured differential cross sections. Some small discrepancies remain at energies between 2 and 3 eV and small scattering angles, where the experimental measurements reveal structure that is not reproduced by the calculations. A more elaborate treatment of the dynamics is evidently needed to describe these features of the differential cross sections in the resonance region.

Acknowledgments

This work was performed under the auspices of the US Department of Energy by the University of California Lawrence Berkeley National Laboratory. The work was supported by the US DOE Office of Basic Energy Science, Division of Chemical Sciences. A.E.O. acknowledges support from the National Science Foundation (Grant No. PHY-99-87877). We are grateful to C. W. McCurdy for helpful discussions.

[1] M. J. Brunger and S. J. Buckman, Physics Reports **357**, 215 (2002).
[2] B. I. Schneider, T. N. Rescigno, B. H. Lengsfield, and C. W. McCurdy, Phys. Rev. Lett. **66**, 2728 (1991).
[3] T. N. Rescigno and B. I. Schneider, Phys. Rev. A **45**, 2894 (1992).
[4] C. Winstead, P. G. Hipes, M. A. P. Lima, and V. McKoy, J. Chem. Phys. **94**, 5455 (1991).
[5] L. M. Brescansin, L. E. Machado, and M. T. Lee, Phys. Rev. A **57**, 3504 (1998).
[6] R. Panajotovic, M. Kitajima, H. Tanaka, M. Jelisavcic, J. Lower, L. Campbell, M. J. Brunger, and S. J. Buckman, J. Phys. B: At. Mol. Opt. Phys. **36**, 1615 (2003).
[7] T. N. Rescigno, C. W. McCurdy, A. E. Orel, and B. H. Lengsfield, *Computational Methods for Electron-Molecule Collisions* (eds. W. M. Huo and F. A. Gianturco, Plenum,

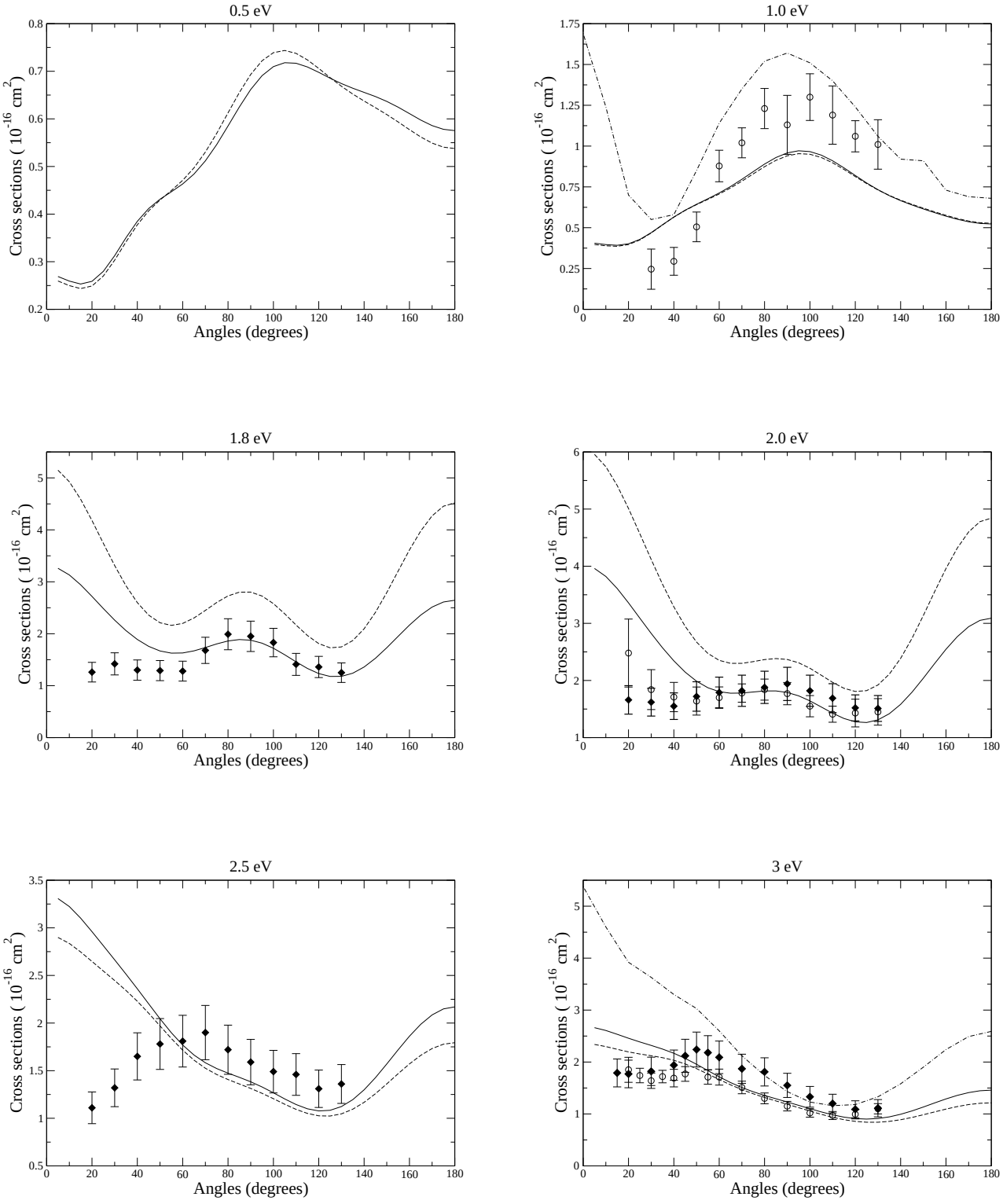

FIG. 5: Elastic differential cross sections for e - C_2H_4 scattering at incident energies 3 eV and below. Solid curves: present results which incorporate an adiabatic-nuclei treatment of symmetric stretch motion. Dashed curves: present results without the inclusion of nuclear motion, at equilibrium geometry. Chained curves: theoretical results of Brescansin *et al.* [5]. Open circles: Panajotovic *et al.* 's ANU measurements [6]. Diamonds: Panajotovic *et al.* 's Sophia measurements [6].

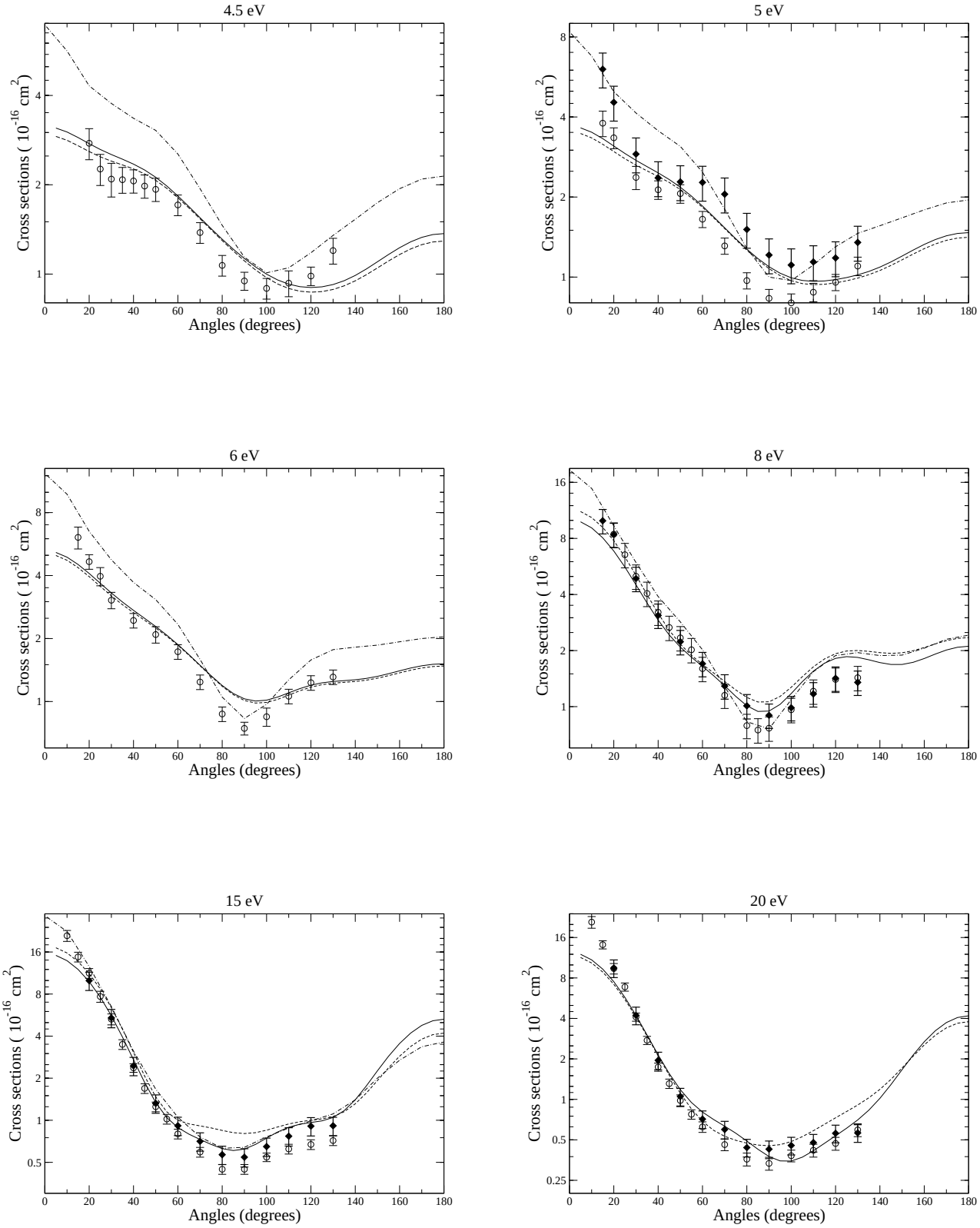

FIG. 6: Elastic differential cross sections for e - C_2H_4 scattering at incident energies above 3 eV. Solid curves: present results which incorporate an adiabatic-nuclei treatment of symmetric stretch motion. Dashed curves: present results without the inclusion of nuclear motion, at equilibrium geometry. Chained curves: theoretical results of Brescansin *et al.* [5].Open circles: Panajotovic *et al.* 's ANU measurements [6]. Diamonds: Panajotovic *et al.* 's Sophia measurements [6].

New York, 1995).
[8] T. N. Rescigno, B. H. Lengsfield III, and C. W. McCurdy, *Modern Electronic Structure Theory*, vol. 1 (ed. D. R. Yarkony, World Scientific, Singapore, 1995).
[9] T. N. Rescigno, D. A. Byrum, W. A. Isaacs, and C. W. McCurdy, Phys. Rev. A **60**, 2186 (1999).
[10] A preliminary version of this work, cited in ref. 6 as a private communication from T. N. Rescigno (2002), used SE results for certain non-resonant symmetries. Those preliminary results should not be considered definitive and differ from the final results presented here.
[11] B. H. Lengsfield III, T. N. Rescigno, and C. W. McCurdy, Phys. Rev. A **44**, 4296 (1991).
[12] W. A. Isaacs, C. W. McCurdy, and T. N. Rescigno, Phys. Rev. A **58**, 309 (1998).
[13] W. A. Isaacs, C. W. McCurdy, and T. N. Rescigno, Phys. Rev. A **58**, 2881 (1998).
[14] G. W. Hills and W. J. Jones, J. Chem. Soc. Faraday Trans. II **71**, 812 (1975).
[15] B. I. Schneider and L. A. Collins, Phys. Rev. A. **30**, 95 (1984).
[16] A. U. Hazi, T. N. Rescigno, and M. Kurilla, Phys. Rev. A **23**, 1089 (1981).
[17] T. N. Rescigno, C. W. McCurdy, and B. I. Schneider, Phys. Rev. Lett. **63**, 248 (1989).
[18] G. Herzberg, *Molecular Spectra and Molecular Structure II. Infrared and Raman Spectra of Polyatomic Molecules* (Van Nostrand Reinhold, 1945).
[19] D. M. Chase, Phys. Rev. **104**, 838 (1956).
[20] M. Allan, Chem. Phys. Letts. **225**, 156 (1994).